Journal of Hazardous Materials 168 (2009) 1047–1052

Contents lists available at ScienceDirect

Journal of Hazardous Materials

journal homepage: www.elsevier.com/locate/jhazmat

Dynamic model for nitric oxide removal by a rotating drum biofilter

Jun Chen, Yifeng Jiang, Jianmeng Chen*, Haolei Sha, Wei Zhang

College of Biological and Environmental Engineering, Zhejiang University of Technology, Hangzhou 310032, China

ARTICLE INFO

Article history:
Received 20 May 2008
Received in revised form 6 January 2009
Accepted 27 February 2009
Available online 11 March 2009

Keywords:
Nitric oxide
Biofilter
Modeling
Anaerobic process
Dynamic simulation
Air pollution control

ABSTRACT

To illustrate the process of nitric oxide (NO) denitrifying removal by a novel rotating drum biofilter (RDB), a dynamic model has been developed and further validated. Based on the mass component profile of NO at the gas–liquid interface combined with a Monod kinetic equation, the model was used to depict the mass transfer-reaction process of NO in RDB, focusing on the concentration distribution of NO in the gas, liquid, and biofilm phases. The NO distribution equation on the biofilm carrier was thereby achieved, as well as a dynamic model for NO elimination in the test system. Additionally, effects of operating parameters such as inlet NO concentration and empty-bed residence time on NO removal efficiency were evaluated through a sensitivity analysis of the model. The model was then modified taking the absorption of NO by nutrition liquid in the bottom of RDB into consideration. The results showed that the simulated data agreed well with the experimental data. The model made it possible to simulate a relatively high NO removal efficiency by RDB.

1. Introduction

As global tropospheric pollution becomes increasingly serious, nitric oxide (NO) emitted from all combustion processes should be brought under strict control. Conventional post-combustion controls for NO abatement include selective catalytic reduction [1], selective non-catalytic reduction [2], adsorption [3], scrubbing [4], and so forth. The biological NO removal from contaminated gas streams was first carried out in the early 1980s [5]. Recently, a new method which combined the advantages of metal chelate absorption and biological reduction was applied to treat NO [6,7]. With low operating cost, no by-product pollution, and its application in large-scale treatment of low-concentration waste gas, biofiltration has been widely accepted as a promising technology in waste gas treatment [8].

Although biofiltration has many advantages over traditional methods, there are also some drawbacks for existing biofilters, such as uneven nutrient distributions, excessive biomass, and media clogging [5]. To solve these problems, an innovative rotating drum biofilter (RDB) has been developed and applied to effectively control the pollution of volatile organic compounds (VOCs), odors [9–11], and NO [12]. However, theoretical studies regarding biofilter modeling are relatively limited, and the kinetics of RDB including biological interactions are not yet well defined [9–13]. In general, first- or zero-order kinetic expressions are always used to describe the biological degradation process [14], and more recently, the Monod kinetic model has been adopted with satisfying results [15,16]. Since the kinetic parameters are essential for the design and optimization of bioreactors, relevant investigations on mathematic models will help researchers to describe and understand the mechanism and dynamics of the NO biodegradation system. Consequently, the biological system of RDB can be designed more scientifically and operated more smoothly to meet various operating conditions.

Biological NO reduction is one of the sequential processes in microbial denitrification, i.e. the respiratory reduction of nitrate to dinitrogen gas (N_2). NO is reduced to dinitrogen with nitrous oxide (N_2O) as intermediate [17]:

$$NO_3^- \rightarrow NO_2^- \rightarrow NO \rightarrow N_2O \rightarrow N_2$$

The reactions are carried out by denitrifiers, which are widely distributed across the bacterial taxa, including *Pseudomonas fluorescens* [18], *P. stutzeri* [19,20], *P. aeruginosa* [21,22] and *Flexibacter canadensis* [23]. These predominantly heterotrophic microorganisms are facultative anaerobes that are able to use NO_3^-, NO_2^- and NO in place of oxygen as an electron acceptor in respiration to cope with low-oxygen or anaerobic conditions. Enzymes involved in the reactions are nitrate reductase, nitrite reductase, nitric oxide reductase and nitrous oxide reductase [24].

The main objective of this study is to develop a dynamic model to predict RDB performance for NO denitrifying removal under anaerobic conditions. Mathematical equations are obtained from overall mass balances including absorption, adsorption, diffusion, and biodegradation. On the basis of the experimental results obtained

* Corresponding author. Fax: +86 571 88320884.
E-mail address: jchen@zjut.edu.cn (J.M. Chen).

0304-3894/$ – see front matter © 2009 Elsevier B.V. All rights reserved.
doi:10.1016/j.jhazmat.2009.02.159

Nomenclature

C_G	NO concentration in gas phase (mg cm^{-3})
C_G^*	NO concentration of liquid–gas interface (mg cm^{-3})
C_L	NO concentration in liquid phase (mg cm^{-3})
C_B	NO concentration in biofilm phase (mg cm^{-3})
C_0	inlet NO concentration (mg cm^{-3})
C_0^*	NO concentration of liquid–gas interface of media (mg cm^{-3})
V_G	gas flow rate (cm s^{-1})
V_L	liquid flow rate in media (cm s^{-1})
a	specific surface area of media (cm^2 cm^{-3})
N_{GL}	mass flux from gas phase to liquid phase (mg cm^{-2} s^{-1})
N_{LB}	mass flux from liquid phase to biofilm phase (mg cm^{-2} s^{-1})
D_G	diffusion coefficient of NO in gas phase (cm^2 s^{-1})
D_L	diffusion coefficient of NO in liquid phase (cm^2 s^{-1})
D_B	diffusion coefficient of NO in biofilm (cm^2 s^{-1})
S	interfacial area (m^2)
r	radial radius (cm)
R_0	outer radius (cm)
R	biological generation rate (mg cm^{-3} s^{-1})
K_S	half-saturation coefficient (mg m^{-3})
X	position in the biofilm (cm)
l	liquid film thickness (cm)
K_L	total transfer coefficient in liquid phase (cm s^{-1})
k_L	transfer coefficient in liquid phase (cm s^{-1})
k_G	transfer coefficient in gas phase (cm s^{-1})
H	solubility constant (kmol kPa^{-1} m^{-3})
E	Henry's constant (MPa)
W	hold-up in the medium (mL)
V	volume of medium (cm^3)
C_1	constant
k_{aq}	NO dissolved rate (mL L^{-1})

Greek symbols

ε_1	porosity of medium (%)
ε_2	proportion of liquid in media (%)
ε_3	proportion of biofilm in media (%)
μ_{max}	maximum growth rate of microorganism (s^{-1})
ρ_B	biomass density in the medium (mg m^{-3})
δ	biofilm thickness (cm)
η	NO removal efficiency (%)

from both gas phase and leachate measurements, we conclude that the dynamic model well simulates the steady-state of the pilot-scale RDB.

2. Materials and methods

2.1. RDB construction and operation

As seen from Fig. 1, the waste gas treatment system was composed of an inlet, inspection port, and the main unit of the RDB. NO waste gas was synthesized using nitrogen and nitric oxide during the operation of the biofilter. A digital mass flow controller ensured an accurate concentration of NO at the inlet of RDB. NO and NO_2 in the inlet and outlet gas flows were measured simultaneously online.

The main unit of RDB consisted of a closed stainless steel chamber in which spongy medium was mounted on a stainless steel drum frame with impermeable plates. The medium was open-pore

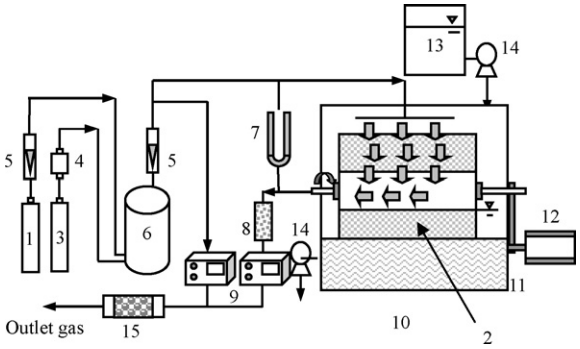

Fig. 1. Schematic representation of the experimental system: (1) N_2 cylinder; (2) packing material; (3) NO cylinder; (4) digital mass meter; (5) rotameter; (6) gas mixing container; (7) pressure meter; (8) dryer; (9) NO/NO_x analyzer; (10) RDB; (11) water temperature control reservoir; (12) motor; (13) nutrient reservoir; (14) metering pump; (15) tail gas absorber.

reticulated polyurethane (PU, Shanghai Xinyuan Sponge Ltd., China) sponge (porosity 93.87%, pore size 2.5 pores cm^{-1}), which was used to support the growth of biofilm in RDB. The axial length of the medium was 10 cm, and the outer and inner diameters were, respectively, 20 cm and 10 cm with a total medium volume of 2.4 L. The bottom of RDB was filled with nutrient solution that enabled the medium and the biofilm to be partly submerged in the solution, and thus allowed the intake of the nutrient by the microorganisms when the rotating drum was rotating through the solution. The total volume of nutrient solution in RDB was kept at 5 L, and was refreshed every 5 days using a tubing pump with a designed rate of 1.0 L day^{-1}.

The experiment was carried out at pH values ranging from 6.5 to 7.5. After entering the working RDB chamber through a dispersion pipe, waste gas passed through the spongy medium coated with the moist microbial biofilm, where the contaminants in the waste gas were absorbed and biodegraded by the biofilm. The purified gas escaped from RDB through the outlet located in the center of the drum.

2.2. Nutrients

The nutrient solution fed to the bioreactor mainly consisted of phosphate and micronutrients as follows: KH_2PO_4 0.5 g L^{-1}, K_2HPO_4 0.5 g L^{-1}, $MgSO_4{\cdot}7H_2O$ 0.1 g L^{-1}, $FeSO_4{\cdot}7H_2O$ 0.1 g L^{-1}, $CuSO_4{\cdot}5H_2O$ 1 mg L^{-1}, $CaCl_2$ 50 mg L^{-1}, and Na_2MoO_4 1 mg L^{-1}. Sodium bicarbonate was used as a buffer to prevent major pH changes in the nutrient solution. Glucose was used as an electron donor and C/N (mole ratio between glucose and NO) of the feeding nutrients was kept at 2.5.

2.3. Bacterial culture

A concentrated sludge was taken from a secondary sedimentation tank at Hangzhou Qige Wastewater Treatment Plant, China. The sludge had been cultured for 2 weeks in a liquid medium (glucose 12,000 mg L^{-1}; sodium nitrate 4800 mg L^{-1}) [25] and then was used for seeding RDB.

2.4. Analytical methods

During the startup and operation of the system, the gas steams were sampled and analyzed. NO and NO_2 concentrations in inlet gas were measured automatically by a Model 42CHL NO–NO_2–NO_x Analyzer (0–5000 mg m^{-3}, Thermo Electron Co., USA), while the concentrations in outlet gas were measured by a Model 42C

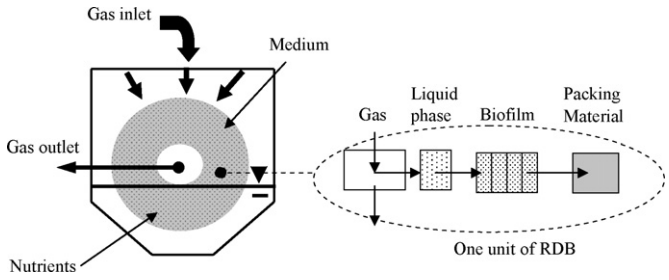

Fig. 2. Typical route of NO transfer in RDB.

$NO–NO_2–NO_x$ Analyzer (0–100 mg m^{-3}, Thermo Electron Co., USA). The pH was analyzed with a Model pHS-9V Acidimeter (Huaguang Wireless Electric Company, Hangzhou, China).

3. Simplified model development

3.1. NO degradation in RDB

Typical route of NO transfer in RDB under anaerobic condition is illustrated in Fig. 2. As NO flows into the RDB, equilibrium is assumed to occur at the gas–biofilm interface, and gaseous and interfacial liquid concentrations are somewhat related to Henry's law. In the biofilm, NO was simultaneously reduced by the denitrifying bacteria into N_2O, then N_2 when it went through the microorganism layer. Fig. 2 illustrates the overall structure taken the mass balances into consideration, while Fig. 3 depicts the modeling details for RDB unit.

Considering the fact that three phases of gas, liquid, and biofilm play roles of reaction media during NO elimination, a mathematical model was developed for the novel biofilter with the aid of mass balance equations. Mass balance equations were proposed on the basis of the following assumptions: (1) RDB rotates stably and any subdivision of the media as defined in Figs. 2 and 3 is identical in terms of both physical and biochemical properties. (2) Equilibrium state of mass transformation is maintained in phase interfaces, and therefore the gas phase interfacial resistance is negligible. (3) Biofilm is mainly on the external surface of the packing material; gas phase reactions occur only in the biofilm phase. (4) Planar geometry and perpendicular diffusion in the biofilm–gas interface can be used to deduce model equations. (5) There is no excessive biomass accumulation in the packing material, and biomass properties are uniform along the drum under different operating conditions. (6) The reaction occurs under anaerobic conditions and the final product is N_2.

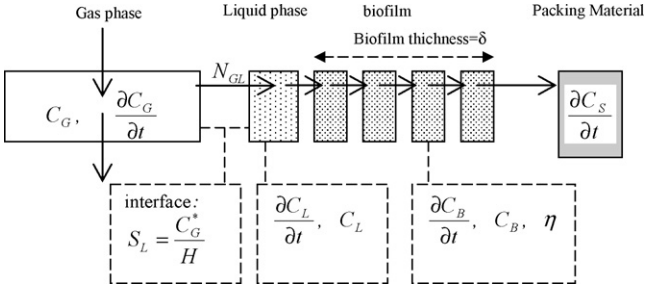

Fig. 3. Schematic description of the model for one unit of RDB. *C* refers to NO concentration, mg cm^{-3}; suffixes *G*/*L*/*B*/*S* refer to gas phase, liquid phase, biofilm, and solid phase respectively; *H* is the NO soluble coefficient, kmol kPa^{-1} m^{-3}; N_{GL} is the mass flux from the gas phase to the liquid phase, mg cm^{-2} s^{-1}; δ is the thickness of biofilm, cm; η is the removal efficiency, %; and *t* is the time, s.

3.2. Dynamic model of NO transfer-biodegration

According to the description above, the transfer process of one RDB unit involved NO diffusion in the gas phase, the mass transfer from the gas phase to the liquid phase, the dissolved and convective diffusion in the liquid phase, the accumulation of mass transfer from the gas phase to the liquid phase, the mass transfer from the liquid phase to the biofilm, and the diffusion and degradation of NO in the biofilm. Mostly, Monod kinetics are assumed as a function of biomass growth and contaminant concentrations [26,27].

Mass balance over the gas phase:

$$\begin{cases} \dfrac{\partial C_G^*}{\partial t} = D_G \dfrac{\partial^2 C_G^*}{\partial r^2} - V_G \dfrac{\partial C_G^*}{\partial r} - \dfrac{a}{\varepsilon_1} N_{GL} \\ r = R_0, \quad C_G^* = C_0^* \end{cases} \tag{1}$$

Mass balance over the liquid phase:

$$\begin{cases} \dfrac{\partial C_L}{\partial t} = D_L \dfrac{\partial^2 C_L}{\partial r^2} - V_L \dfrac{\partial C_L}{\partial r} + \dfrac{a}{\varepsilon_2} N_{GL} - \dfrac{a}{\varepsilon_2} N_{LB} \\ N_{LB} = -D_B \left(\dfrac{\partial C_B}{\partial X} \right) | X = 0 \end{cases} \tag{2}$$

Mass balance over the biofilm:

$$\begin{cases} \dfrac{\partial C_B}{\partial t} = D_B \dfrac{\partial^2 C_B}{\partial X^2} - \mu_{\max} \times \rho_B \times \dfrac{C_L}{K_S + C_L} \\ X = 0, \quad C_B = C_L \\ -D_B \left(\dfrac{\partial C_B}{\partial X} \right) | X = \delta = -D_B \left(\dfrac{\partial C_S}{\partial X} \right) | X = \delta \end{cases} \tag{3}$$

In NO elimination, the microorganism species in biofilm are complex [28,29], but can be assumed as one kind of microorganism according to the model developed by Grady et al. [30]. The parameters of the model are therefore considered to be one kind of microorganism. Hunik et al. [31,32] reported that when the microorganism metabolized the inorganic compounds, such as NO_2, NH_3, NO_2^-, and so forth, the reaction is a zero-order reaction, with its half-saturation coefficient between 0.1 and 1.0 mg L^{-1}. Catton et al. [33] shared the same opinion and reported that the removal efficiency would not be influenced by the increasing NO concentration at low concentrations (<600 mg m^{-3}), with mass transfer being the key limiting factor. In this investigation, the NO concentration is below 8.04×10^{-4} mg cm^{-3}, so the following inference can be achieved.

Besides, the two-phase resistance theory postulates that the overall resistance to interfacial mass transfer is equal to the sum of the individual liquid- and gas-phase resistances, therefore,

$$\frac{1}{K_L} = \frac{H}{k_G} + \frac{1}{k_L} \tag{4}$$

$$C_L = \frac{k_L}{k_L + \delta k_1} \times C_G^* \tag{5}$$

Eqs. (1)–(5) can be rewritten as

$$V_G \frac{\partial C_G^*}{\partial r} = \frac{K_L a}{\varepsilon_1} \left(C_G^* - \frac{k_L}{k_L + \delta k_1} \times C_G^* \right) = \frac{k_L a \delta k_1}{\varepsilon_1 (k_L + \delta k_1)} \times C_G^* \tag{6}$$

Subject to:

$$\frac{a}{\varepsilon_1} N_{GL} = \frac{K_L a}{\varepsilon_1} (C_G^* - C_L)$$

$$C = \frac{k_L a \delta k_1}{\varepsilon_1 (k_L + \delta k_1) V_G}, \tag{7}$$

Table 1
Parameter values used for solving the model equations.

Parameter and symbol	Value	Unit	Reference
Porosity of the medium, ε	0.94		Experimental determination
Biofilm thickness, δ	0.1	cm	[16,43]
Diffusion coefficient in the liquid phase, D_L	2.32×10^{-5}	$cm^2\ s^{-1}$	[33]
Diffusion coefficient in the gas phase, k_G	2×10^{-4}	$mol\ cm^{-2}\ s^{-1}\ MPa^{-1}$	[34]
Half-saturation coefficient, K_S	1.0×10^{-4}	$mg\ cm^{-3}$	[33]
Mass transfer coefficient, k_L	1.98×10^{-3}	$cm\ s^{-1}$	[34]
Dissolution coefficient, H	1.91×10^{-5}	$kmol\ kPa\ m^{-3}$	[34]
Biomass density, ρ_B	1.0	$g\ cm^{-3}$	Experimental determination

$$\delta k_1 \gg k_L, \quad H \gg k_G \tag{8}$$

$$\varepsilon_1 = \varepsilon - \varepsilon_2 - \varepsilon_3 = \varepsilon - \frac{W}{V} - a\delta \tag{9}$$

When $r = R_0$ and $C_G^* = C_0^*$, the pollutant distribution equation in the dimensionless form of the drum is

$$C_G = C_0 \exp\left[-\frac{k_L a}{\varepsilon_1 V_G}(R_0 - r)\right] \tag{10}$$

According to Cussler [34], $k_L = D_L aV/W$, so the pollutant distribution equation in the drum can be inferred as

$$C_G = C_0 \exp\left[-\frac{D_L a^2 V}{\left(\varepsilon - W/V - a\delta\right) W V_G}(R_0 - r)\right] \tag{11}$$

Along the radial direction of RDB, the removal efficiency can be inferred as

$$\eta = \frac{C_0 - C_G}{C_0} = 1 - \frac{C_G}{C_0} \tag{12}$$

4. Results and discussion

In the following investigation, the simplified model obtained is applied for the dynamic simulation of a realistic operating case and further examined with respect to its parametric sensitivity. The values of the model parameters selected for NO treatment are listed in Table 1.

4.1. Effect of inlet NO concentration on NO removal efficiency

Fig. 4 represents the effects of inlet NO concentration on the removal efficiency. The experimental and model simulated removal efficiencies showed similar trends, but the former was 10% higher than the latter under the operating conditions of EBRT 65 s and rotating speed 0.5 rpm. The simplified model could predict the performance of RDB for NO removal. As shown in Fig. 4, with the inlet NO concentration increasing, the biofilm had the potential to eliminate the additional NO loading when the nutrition was sufficient for the enhancement of bacteria growth. Biofilm therefore could degrade NO more rapidly at the higher inlet pollutant concentration due to the improved mass diffusion and reaction dynamics. However, on the other hand, the inlet NO concentration increased faster than elimination capacity of bacteria, and it led to the continuous drop in NO removal efficiency. The reasons for this phenomenon were that: (1) with the inlet NO concentration increasing, the degradation time of NO by biofilm became shorter; (2) bacteria on the biofilm grew faster, resulting in clogging in some parts of the media, which influenced the elimination capacity.

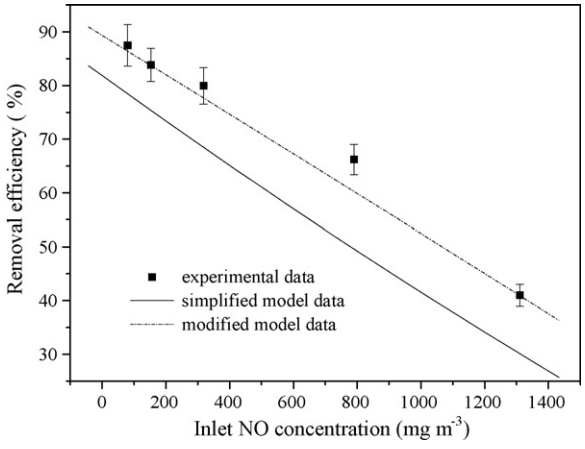

Fig. 4. Removal efficiency comparisons between model results and experiment data at different inlet NO concentrations.

The main reasons for the difference between the experimental and simulated profiles can be listed as follows: (1) in order to maintain the microorganism metabolism, parts of the nutrient liquid were kept in the bottom of the drum. As a result, the lower simulated profiles could be induced by neglecting the absorption of NO and following denitrification in the nutrient liquid. In addition, the nutrient liquid flow rate increased with the rotation of the medium, and the reduction of NO through absorption was consequently enhanced. (2) In the assumptions, the water layer was regarded to be still and equilibrium over the surface of media was uniform. In fact, the water flowed downwards because of gravity, so that most of the hold-up liquid remained in the inner medium. So the inner water layer was thicker than the outer layer, and the distribution of outer microorganisms over the medium was therefore denser than that of the inner. It showed that the outer microorganisms actually removed most of NO. Accordingly, the transfer resistance coefficient increased during the modeling process, which contributed to the decrease of removal efficiency. (3) According to the surface renew theory, $K_C = \sqrt{SD_{AB}}$ [35], the flow of liquid could enlarge the mass transfer coefficient. But in the modeling process, the liquid was regarded as stationary, and thus the simplified model predictions were lower than the experimental profiles.

4.2. Effect of EBRT on NO removal efficiency

EBRT is an important parameter for the bioreactor design. Optimal EBRT, which corresponds to a certain proper gas flow rate (V_G), will be beneficial to NO removal. Fig. 5 illustrates the difference between the experimental and simulated profiles at inlet NO concentration of 344 $mg\ m^{-3}$ and drum rotating speed of 0.5 rpm.

The results showed that the model simulated profiles were 10% lower than the experimental profiles, which coincided with the results on the effect of inlet NO concentration. The incongruity with the effect of drum rotation is that at short EBRT, the difference enlarges to 20%, while it decreases to 10% at high EBRT. The reasons are as follows.

(1) The difference between experimental and simulated profiles is attributed to the neglect of absorption and the effect of hold-up liquid of RDB.

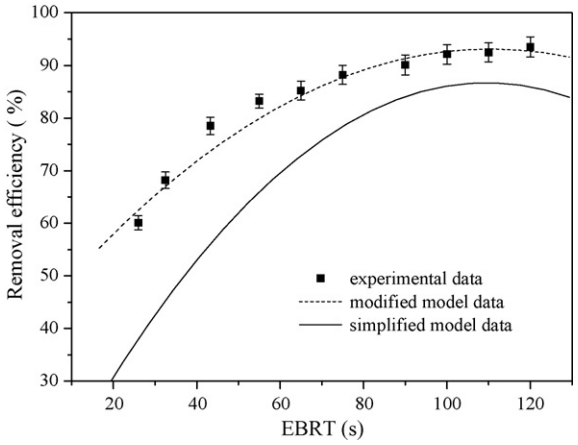

Fig. 5. Removal efficiency comparisons between model results and experiment data at different EBRTs.

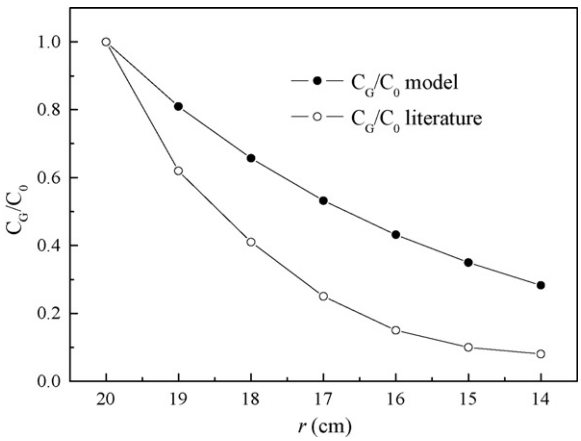

Fig. 6. NO concentration distribution along the radius of RDB.

(2) Under the conditions of short EBRT and high gas flow rate, the effect of absorption is strengthened, which contributed to the difference between the experimental and simulated profiles.

4.3. Model modification

Based on the above analysis, the chemical absorption and biological reduction of NO by nutrition liquid in the bottom of RDB could not be ignored. The rapid and quantitative NO dissolved in the aqueous solution to HONO/NO_2^- had been used to analyze the dissolution of NO in water [36,37]. Glasson and Tuesday [38] established both the stoichiometry (Eq. (13)) of this reaction and the rate law for the appearance of NO (Eq. (14)) in aqueous phase. Zhang et al. [39] reported that NO had low solubility in the water, while the NO_2^- production in the water could be rapidly denitrified to N_2 by denitrifiers in the drum [40]. Therefore, the NO transfer limited process was more important than the reaction limited process for the NO removal process

$$NO + H_2O \rightarrow NO_2^- + 2H^+ \quad (13)$$

$$C_L = \frac{k_{aq}}{k_{aq} + Sk_1} \times C_0 \quad (14)$$

According to Dean [41], the NO dissolved rate $k_{aq} = 0.043\ \mathrm{ml\,L^{-1}}$ under the condition of 101.325 kPa and 25 °C.

So the pollutant distribution equation (11) in the drum could be rewritten as follows:

$$C_G = C_0 \exp\left[-\frac{D_L a^2 V}{\left(\varepsilon - (W/V) - a\delta\right) WV_G}(R_0 - r)\right] - \frac{k_{aq}}{k_{aq} + Sk_1} \times C_0 \quad (15)$$

The comparison between the modified model data and the experimental data of NO removal by RDB could be seen in Figs. 4 and 5. It showed that the calculated values were in well accordance with the experimental values.

4.4. Prediction of NO distribution on the drum

Fig. 6 illustrates that the NO concentration distribution along the different radius of the packing materials under the conditions of EBRT of 65 s, drum rotating speed at 0.5 rpm, and inlet NO concentration of 344 $\mathrm{mg\,m^{-3}}$.

Due to the restriction of detection methods, the NO concentration along the radius direction in RDB could not be measured in this study. From Fig. 6, the NO concentration of the model gradually decreased along the radius of medium, but the tendency was more rapid in the outer medium in relation to the inner medium. This demonstrated that the NO degradation rate along drum radius agreed well with pollutant mass transfer model and removal kinetics of the biofilm. Under the same operational conditions, the simulative calculation of traditional biofilter model [42] was compared with that of RDB model. As shown in Fig. 6, the NO concentration curve along the radius of packing materials of RDB was flatter than that of the traditional biofilter, which indicated the lower mass transfer resistance of NO in RDB and higher effective utility of packing materials. The above results suggest that the novel RDB have more advantages over traditional bioreactors in terms of high even distribution of biomass and no biomass clogging of packing materials.

5. Conclusions

The investigation analyzed the process of transfer-reaction of NO in RDB. Based on the mass balance of pollutants in gas, liquid, and biofilm phases, a dynamic model was put forward to describe the NO concentration distribution in RDB and the NO removal efficiency. The predictions of theoretical model under steady-state conditions agreed well with the experimental data under low NO concentrations (<600 $\mathrm{mg\,m^{-3}}$) treated in RDB. Then, the model was further modified in consideration of the NO absorption and following denitrification by nutrition liquid in the drum. Due to the lower mass transfer resistance and higher effective utility of packing materials, RDB was also proved as a stable and suitable process for NO denitrification in comparison with traditional bioreactors.

Acknowledgement

The research was funded by the National Natural Science Foundation of China (No. 20776134).

References

[1] M. Bradford, R. Grover, P. Paul, Controlling NOx emissions: Part 1, Chem. Eng. Prog. 98 (3) (2002) 42–46.
[2] M. Bradford, R. Grover, P. Paul, Controlling NOx emission: Part 2, Chem. Eng. Prog. 98 (4) (2002) 38–42.
[3] C.B. Wang, T.F. Yeh, H.K. Lin, Nitric oxide adsorption and desorption on alumina supported palladium, J. Hazard. Mater. 92 (3) (2002) 241–251.
[4] H. Chu, T.W. Chien, B.W. Twu, The absorption kinetics of NO in $NaClO_2$/NaOH solutions, J. Hazard. Mater. 84 (2–3) (2001) 241–252.
[5] Y.M. Jin, M.C. Veiga, C. Kennes, Bioprocesses for the removal of nitrogen oxides from polluted air, J. Chem. Technol. Biotech. 80 (5) (2005) 483–494.

[6] W. Li, C.Z. Wu, Y. Shi, Metal chelate absorption coupled with microbialreduction for the removal of NOx from flue gas, J. Chem. Technol. Biotech. 81 (2006) 306–311.
[7] W. Li, C.Z. Wu, S.H. Zhang, K. Shao, Y. Shi, Evaluation of microbial reduction of Fe(III)EDTA in a chemical absorption—biological reduction integrated NOx removal system, Environ. Sci. Technol. 41 (2007) 639–644.
[8] J.S. Devinny, J. Ramesh, A phenomenological review of biofilter models, Chem. Eng. J. 113 (2–3) (2005) 187–196.
[9] B. Kim, X. Zhu, M. Suidan, An innovative biofilter for treating VOCs in air emissions, in: Proceedings of the Air and Waste Management Association's 95th Annual Conference, Baltimore, 2002.
[10] C.P. Yang, M.T. Suidan, X. Zhu, B.J. Kim, Comparison of single-layer and multilayer rotating drum biofilters for VOC removal, Environ. Prog. 22 (2) (2003) 87–94.
[11] C.P. Yang, M.T. Suidan, X. Zhu, B.J. Kim, Removal of a volatile organic compound in a hybrid rotating drum biofilter, J. Environ. Eng. 130 (3) (2004) 282–291.
[12] J.D. Wang, C.Q. Wu, J.M. Chen, H.J. Zhang, Denitrification removal of nitric oxide in a rotating drum biofilter, Chem. Eng. J. 121 (1) (2006) 45–49.
[13] C.P. Yang, M.T. Suidan, X. Zhu, B.J. Kim, Biomass accumulation patterns for removing volatile organic compounds in rotating drum biofilters, Water Sci. Technol. 48 (8) (2003) 89–96.
[14] S.P.P. Ottengraf, A.H.C. Van Den Oever, Kinetics of organic compound removal from waste gases with a biological filter, Biotechnol. Bioeng. 25 (12) (1983) 3089–3102.
[15] S.M. Zarook, A.A. Shaikh, Z. Ansar, Development, experimental validation and dynamic analysis of a general transient biofilter model, Chem. Eng. Sci. 52 (5) (1997) 759–773.
[16] M.A. Deshusses, G. Hamer, I.J. Dunn, Behavior of biofilters for waste air biotreatment. 1. Dynamic model development, Environ. Sci. Technol. 29 (4) (1995) 1048–1058.
[17] I.M. Wasser, S. de Vries, P. Moenne-Loccoz, I. Schroder, K.D. Karlin, Nitric oxide in biological denitrification: Fe/Cu metalloenzyme and metal complex NOx redox chemistry, Chem. Rev. 102 (4) (2002) 1201–1234.
[18] M.K. Firestone, R.B. Firestone, J.M. Tiedje, Nitric-oxide as an intermediate in denitrification—evidence from N-13 isotope exchange, Biochem. Biophys. Res. Commun. 91 (1) (1979) 10–16.
[19] K. Frunzke, W.G. Zumft, Inhibition of nitrous-oxide respiration by nitric oxide in the denitrifying bacterium *Pseudomonas perfectomarina*, Biochem. Biophys. Acta 852 (1) (1986) 119–125.
[20] F. Schafer, R. Conrad, Metabolism of nitric-oxide by *Pseudomonas stutzeri* in culture and in soil, FEMS Microbiol. Ecol. 102 (2) (1993) 119–127.
[21] I. Kalkowski, R. Conrad, Metabolism of nitric-oxide in denitrifying *Pseudomonas aeruginosa* and nitrate-respiring *Bacillus cereus*, FEMS Microbiol. Lett. 82 (1) (1991) 107–111.
[22] R. Vosswinkel, I. Neidt, H. Bothe, The production and utilization of nitric-oxide by a new, denitrifying strain of *Pseudomonas aeruginosa*, Arch. Microbiol. 156 (1) (1991) 62–69.
[23] Q.T. Wu, R. Knowles, Y.K. Chan, Production and consumption of nitric-oxide by denitrifying *Flexibacter canadensis*, Can. J. Microbiol. 41 (7) (1995) 585–591.
[24] L.I. Hochstein, G.A. Tomlinson, The enzymes associated with denitrification, Annu. Rev. Microbiol. 42 (1988) 231–261.
[25] R.R. Nair, P.B. Dhamole, S.S. Lele, S.F. D'Souza, Biological denitrification of high strength nitrate waste using preadapted denitrifying sludge, Chemosphere 67 (8) (2007) 1612–1617.
[26] W. Den, M. Pirbazari, Modeling and design of vapor-phase biofiltration for chlorinated volatile organic compounds, AIChE J. 48 (9) (2002) 2084–2103.
[27] A.R. Dincer, F. Kargi, Kinetics of sequential nitrification and denitrification processes, Enzyme Microb. Technol. 27 (1–2) (2000) 37–42.
[28] J.A. Steele, F. Ozis, J.A. Fuhrman, J.S. Devinny, Structure of microbial communities in ethanol biofilters, Chem. Eng. J. 113 (2–3) (2005) 135–143.
[29] S. Yoshie, N. Noda, T. Miyano, S. Tsuneda, A. Hirata, Y. Inamori, Microbial community analysis in the denitrification process of saline-wastewater by denaturing gradient gel electrophoresis of PCR-amplified 16S rDNA and the cultivation method, J. Biosci. Bioeng. 92 (4) (2001) 346–353.
[30] C.P.L. Grady, G.T. Daigger, H.C. Lim, Waste Water Bio-treatment, Chemical Industry Press, Beijing, 2003.
[31] J.H. Hunik, J. Tramper, R.H. Wijffels, A strategy to scale up nitrification processes with immobilized cells of *Nitrosomonas europaea* and *Nitrobacter agilis*, Bioprocess. Eng. 11 (2) (1994) 73–82.
[32] J.H. Hunik, H.J.G. Meijer, J. Tramper, Kinetics of *Nitrobacter agilis* at extreme substrate, product and salt concentrations, Appl. Microbiol. Biotechnol. 40 (2–3) (1993) 442–448.
[33] K. Catton, L. Hershman, D.P.Y. Chang, J.M. Chen., Aerobic removal of NO on carbon foam packings, in: Proceedings of the 95th Air and Waste Management Association Annual Conference, Baltimore, 2002.
[34] E.L. Cussler, Diffusion Mass Transfer in Fluid Systems: Mass Transfer in Fluid Systems, Cambridge University Press, 1997, pp. 144.
[35] G. Astarita, Mass Transfer with Chemical Reaction, Elsevier, New York, 1970.
[36] V.G. Kharitonov, A.R. Sundquist, V.S. Sharma, Kinetics of nitric-oxide autoxidation in aqueous-solution, J. Biol. Chem. 269 (8) (1994) 5881–5883.
[37] V.R. Shenoy, J.B. Joshi, Kinetics of oxidation of aqueous sulfite solution by nitric-oxide, Water Res. 26 (7) (1992) 997–1003.
[38] W.A. Glasson, C.S. Tuesday, The atmospheric thermal oxidation of nitric oxide, J. Am. Chem. Soc. 85 (1963) 2901–2904.
[39] S.H. Zhang, X.H. Mi, L.L. Cai, J.L. Jiang, W. Li, Evaluation of complexed NO reduction mechanism in a chemical absorption—biological reduction integrated NOx removal system, Appl. Microbiol. Biotechnol. 79 (4) (2008) 537–544.
[40] P.G. Lee, R.N. Lea, E. Dohmann, W. Prebilsky, P.E. Turk, H. Ying, J.L. Whitson, Denitrification in aquaculture systems: an example of a fuzzy logic control problem, Aquacult. Eng. 23 (1–3) (2000) 37–59.
[41] J.A. Dean, Lange's Handbook Chemistry, McGraw Hill Inc., New York, 1999.
[42] G. Baquerizo, J.P. Maestre, T. Sakuma, M.A. Deshusses, X. Gamisans, D. Gabriel, J. Lafuente, A detailed model of a biofilter for ammonia removal: model parameters analysis and model validation, Chem. Eng. J. 113 (2–3) (2005) 205–214.
[43] M.A. Deshusses, G. Hamer, I. Dunn, Behavior of biofilters for waste air biotreatment. 1. Dynamic model development, Environ. Sci. Technol. 29 (1995) 1048–1058.